

Development of PEG-mediated Genetic Transformation and Gene Editing System of *Bryum argenteum* as a Abiotic Stress Tolerance Model Plant

Fengjun Leng (✉ 2200801015@cnu.edu.cn)

Capital Normal University <https://orcid.org/0009-0007-2326-9079>

Guiwei Zhou

Capital Normal University

Ruoyuan Shi

Capital Normal University

Chengyang Liu

Capital Normal University

Yirui Lin

Capital Normal University

Xinqiang Yu

Capital Normal University

Yanhua Zhang

Capital Normal University

Xiangxi He

Capital Normal University

Zhu Liu

Capital Normal University

Fang Bao

Capital Normal University

Yong Hu

Capital Normal University <https://orcid.org/0009-0003-7665-3542>

Yikun He

Capital Normal University

Research Article

Keywords: *Bryum argenteum*, protoplasts, PEG-mediated transformation, CRISPR/Cas9 system, ABI3.

Posted Date: September 25th, 2023

DOI: <https://doi.org/10.21203/rs.3.rs-3331235/v1>

License:  This work is licensed under a Creative Commons Attribution 4.0 International License.

[Read Full License](#)

Version of Record: A version of this preprint was published at Plant Cell Reports on February 10th, 2024.

See the published version at <https://doi.org/10.1007/s00299-024-03143-9>.

Abstract

Bryum argenteum is a fascinating, cosmopolitan, and versatile moss species that thrives in various disturbed environments. Because of its comprehensive tolerance to desiccation, high UV and extreme temperatures, it is emerging as a model moss for studying the molecular mechanisms underlying the responses of plants to abiotic stresses. However, due to the lack of basic tools such as gene transformation, targeted genome modification, molecular mechanisms underlying the survival of *B. argenteum* in different environments are poorly understood. Here, we reported the protonema of *B. argenteum* can survive up to 95.42% water loss. The genome size of *B. argenteum* is approximately 313 Mb by kmer analysis, smaller than reported 700 Mb. Then, we established a simple method for protonema induction and an efficient protoplast isolation and regeneration protocol for *B. argenteum*. Moreover, a PEG-mediated *B. argenteum* protoplast transient transfection and stable transformation system was developed. Two homologues of *ABI3*(ABA-INSENSITIVE 3) gene were cloned from *B. argenteum*. This genetic transformation system was further optimized for CRISPR/Cas9 system for targeted delivery of the *BaABI3A* and *BaABI3B* gene into *B. argenteum* protoplasts, which triggered mutagenesis at the target in about 2%-5% of the regenerated plants. Isolated *ABI3A* and *ABI3B* mutants are all sensitive to desiccation, which suggested *BaABI3A* and *BaABI3B* play redundant roles in desiccation stress. Our results provide a rapid and simple approach for molecular genetics in *B. argenteum*. The results of this study will help to understand the molecular mechanisms of plant extreme environmental adaptation.

Key message

To establish a sterile culture system and protoplast regeneration system for *Bryum argenteum*, and to establish and apply CRISPR/Cas9 system in *Bryum argenteum*

Introduction

Bryophyte, including liverworts, moss and hornworts, belong to an independent species within the higher plants and are an essential group for transitioning from aquatic to terrestrial plants, with all land plants being its sister group, including the classes *Bryopsida*, *Andreaeopsida*, and *Takakiopsida* (Puttick et al., 2018; Sousa et al., 2019). Unlike vascular plants, the gametophyte generation is the dominant generation in the life cycle of bryophyte plants. These unique characteristics make it easier to study functional genomics through homologous recombination and CRISPR technology to obtain mutants (Wiedemann et al., 2010; Ponce de León and Montesano, 2013; Lopez-Obando et al., 2016; Collonnier et al., 2016; Ikeda et al., 2018; Trogu et al., 2020).

Bryum argenteum, dioecism, is a fascinating and versatile moss species because it can be widely distributed in arid, humid, high UV and urban environments (Gao et al., 2017; Pisa et al., 2014; Hui et al., 2013; Shaw et al., 1989; Shaw et al., 1990; Schroeter et al., 2012; Zaccara et al., 2020). This typical drought-tolerant moss resurrection plant can achieve dehydration of more than 95% and rapidly recover

within a few seconds when rehydrated. As an extremely desiccation-tolerant moss, *B. argenteum* can survive under extremely dry air conditions (i.e., 0–30% RH or less than 162 MPa), and it is classified as category “A” among the most desiccation tolerant (DT) moss species (Wood, 2007). While *Physcomitrium Patens* as a moss model, which was recently renamed from *Physcomitrella patens*, only can survive up to 92% water loss but cannot recover from complete desiccation (Frank et al., 2005; Khandelwal et al., 2010). *B. argenteum* is dioecious with apparent alternation of generations and can be spread by spores produced through sexual reproduction over short or long distances, as well as by short-distance asexual reproduction through gemmae. Phenotypic plasticity has been shown to have ecotype-wide thermotolerance in *B. argenteum*, which can reasonably be expected to have plasticity in other physiological traits (He et al., 2016). There are also reports on the drought tolerance of *B. argenteum* (Greenwood et al., 2019), the establishment of spore in vitro culture conditions (Sabovljević et al., 2005), and the effects of plant hormones in vitro development (Sabovljević et al., 2010), as well as reports on the cultivation of its protonema and gametophyte (Pandey et al., 2014). However, research on *Bryum argenteum* is still in its early stages. In addition, *B. argenteum* lacks basic tools such as gene transformation and genome editing technologies, which limits the study of its unique characteristics.

To survive on land, the earliest land plants had to develop mechanisms to tolerate desiccation. The phytohormone abscisic acid (ABA) protects seeds in angiosperm and vegetative tissues in moss during water stress by activating genes through transcription factors such as ABSCISIC ACID INSENSITIVE 3 (*ABI3*) (Meurs et al., 1992). *ABI3* belongs to the plant-specific B3 DNA binding domain protein family. B3 domain-containing proteins are divided into five major categories, including the *REM* (reproductive meristem) subfamily, *HIS* family (high-level expression of sugar inducible), *ARF* family (auxin response factor), *RAV* family (related to *ABI3/VP1*), and *ABI3* family. Compared with other B3 domain transcription factor families, the *ABI3* family is relatively small and evolutionarily conserved. *ABI3* is a core component of the ABA signaling pathway and was initially thought to be a seed-specific transcription factor that controls seed maturation and the onset of dormancy. However, subsequent studies have shown that *ABI3* expression plays a role in cell differentiation in nutrient tissues, increases dehydration tolerance, degrades chlorophyll, and extends seed lifespan (Zhang et al., 2018). *ABI3* also plays a role in the induced dehydration tolerance of *P. patens* (Khandelwal et al., 2010), suggesting that this transcription factor may have a more conserved role in the evolution of non-biological stress tolerance in land plants (Marella et al., 2006; Takezawa et al., 2011).

The advent of sequence-specific nucleases capable of genome editing is revolutionizing basic and applied biology. Since the introduction of CRISPR-Cas9, genome editing has been widely used in transformable plants to characterize gene function and improve trait. Because of its low cost, simplicity, and high efficiency, the CRISPR-Cas system has become the most widely used system for plant genome editing (Yin et al., 2017). This technology has been rapidly expanding and applied to major cereals such as rice, wheat, and maize (*Zea mays*) and to other crops that are important for food security, such as potato (*Solanum tuberosum*) and cassava (*Manihot esculenta*) (Chen et al., 2019; Zhu et al., 2020; Gao, 2021), which helps secure global food supplies. However, CRISPR-Cas is capable of <https://>doing more than just editing specific genetic loci to improve crops. Among non-vascular plants, such as bryophytes:

P.patens, *Marchantia polymorpha*, CRISPR-Cas system has also been used to explore the molecular mechanisms underlying the transition from aquatic to terrestrial pioneer plants.

B. argenteum has gained increasing attention as a model organism for desiccation tolerance due to its comprehensive tolerances to the drought, extreme temperatures and high UV, so it is important for *B. argenteum* to create its molecular biology methods. In this study, we chose cosmopolitan and versatile *B. argenteum* as our research model materials (<http://www.discoverlife.org/mp/20m?kind=Bryum+argenteum>). We first explored the drought tolerance of *B. argenteum* and the ecotypes of *B. argenteus* in different hydroponic environments for the first time. Next, we investigated the impact of the protoplast isolation time on *B. argenteum* and observed the protoplast regeneration system. By optimizing the *Physcomitrium patens* transformation strategy, we developed a transient transformation and a stable transformation method for *B. argenteum*. In addition, we also established a genome editing method for *B. argenteum* using CRISPR/Cas9 technology and investigated the function of the two *ABI3* homologue genes in this species. The establishment of *B. argenteum* transformation method has multiple uses, such as identifying the molecular mechanisms by which *B. argenteum* adapts to diverse environments worldwide and developing more medicinal and economic value products from *B. argenteum*.

Materials & Methods

Plant Collection and Culture

The gametophyte or capsula of *B. argenteum* was collected from various regions across the country, naturally dried, and brought back to the laboratory for aseptic treatment. The collected gametophyte materials were washed several times with tap water, separated into individual plants, and placed on moist, sterile filter paper. The single stem tips were sterilized with different gradients of NaClO (5%, 10%, 15%) for 1 min, 2 min, or 5 min. After sterilization, the moss was inoculated onto a sugar-free BCD solid culture medium and grown in a culture box at 22°C, with a light cycle of 16 hours light/8 hours dark and a light intensity of 50 $\mu\text{E/s}$.

It is important to establish a stable protonema culture system for moss genetics transformation. To observe the protonema growth of *B. argenteum* in liquid BCD, we used BCD as the primary medium (Zhao et al., 2018), adding glucose as the carbon source, and adding ammonium tartrate as the nitrogen source. We prepared four media with different carbon and nitrogen sources: carbon + nitrogen, no carbon + nitrogen, carbon + no nitrogen, and no carbon + no nitrogen. The stem and leaf of *B. argenteum* were suspended in a liquid medium on a shaker at 120 rpm/min, 25°C, with a light cycle of 16 h/8 h and light intensity of 100 $\mu\text{E/s}$. The growth of stem and leaf, as well as protonema, were observed.

Phylogenetic Analysis

The total genomic DNA was extracted from the protonema of *B. argenteum* using the CTAB method (Byun et al., 2021). The extracted genomic DNA was used as the template for PCR analysis with a reaction

system consisting of 1 ul of genomic DNA template, 1 ul of 10 uM forward and reverse primers, and 25 ul of PCR Master Mix (Novozymes). The amplification program was as follows: pre-denaturation at 98°C for 3 min, denaturation at 98°C for 10 s, annealing at 58°C for 20 s, and extension at 72°C for 30 s/Kb. The primer sequences were used to amplify *trnL-F*, *trnG*, *atpB-rbcL*, *nad5*, and *26S* and are listed in Supplementary Table S1. To construct a phylogenetic tree including *B. argenteum*, the concatenated sequences of *trnL-F*, *trnG*, *atpB-rbcL*, *nad5*, and *26S* were compared with the concatenated sequences of other species (obtained from GeneBank) (Taberlet et al., 1991; Pedersen N et al., 2006 Table 1). The sequences were aligned using Bioedit software, and downstream analysis was performed using IQ-TREE program and Figtree. A maximum likelihood method was used to construct the phylogenetic tree, and 1000 bootstrap replicates were used to test the support for internal branches.

Estimation of Genome Size

DNA samples were broken into fragments with a length of 300 bp by an ultrasonic disruptor. DNA library was constructed and subjected to Paired-end sequencing using the Illumina HiSeq sequencing platform. Finally, clean reads were used to estimate the genome size using K-mer frequency (K-mer 17 bp).

Protoplast Isolation

A strain CNU51 of female material obtained from capsula collected by in Capital Normal University in Beijing, China (N39°9'E116°3', 2015) was used as the model material for protoplast isolation.

Using 8% of mannitol buffer and enzyme concentration for protoplast isolation based on the moss *P. patens* method (Collonnier et al., 2016 Hohe et al., 2004) as a reference, 0.8% driselase was dissolved in 8% mannitol and rotated gently at 4°C to isolate protoplasts. Transfer protonema to a petri dish and mix carefully with a 0.8% driselase solution (Sigma), dissolved in 8% mannitol. Place in darkness on a tumble shaker at low speed. After 10min, 20min, 30min, 40min, 50min, the sample were observed. All further steps follow the protocol described in Hohe et al. (2004) and have been adapted considering protoplast density and regeneration. The isolated protoplasts were centrifuged at 200 rcf for 2 min at 4°C, the supernatant-containing enzyme was removed, and the protoplasts were resuspended in 8% mannitol and centrifuged again. This process was repeated twice, and the protoplasts were collected and finally counted and subjected to PEG transformation using a 3 M mannitol solution.

RT-PCR Analysis

Total RNA was extracted from protonema tissue using a classic TRIzol method with some modifications by RNA adsorption column (TIANGEN). The quantity and quality of RNAs were determined by spectroscopic analysis using a NanoDrop Lite Spectrophotometer (Thermo Scientific, United States) and agarose gel electrophoresis. First-strand cDNA was synthesized from 500 ng of total RNA using using Prime-Script® RT Reagent Kit with gDNA Eraser (TaKaRa, Shiga, Japan). RT-PCR analysis was performed in 10 µL reactions containing adjusted cDNA template, 10 µM of each primer, and 5 µL of Taq master mix (Vazyme). The amplification procedure was as follows: 5 min of denaturation and enzyme

activation at 95°C followed by 28 cycles at 95°C for 15 s, 58°C for 15 s, and 72°C for 15 s. The actin gene was used as an internal control. The DNA sequences of the primers used for PCR amplification are listed in Supplementary Table S1.

RT-qPCR Analysis

The dynamic transcript levels of the GFP gene were analyzed by RT-qPCR. The cDNA is derived from the RT-PCR analysis described above. The sample mixture of RT-qPCR was prepared based on the procedures described in TB Green® Premix Ex Taq™ II (Tli RNaseH Plus) (TaKaRa, Shiga, Japan). The relative expression levels of GFP were calculated using the comparative threshold cycle method $2^{-\Delta\Delta CT}$ (Livak and Schmittgen, 2001).

Immunoblot assay

Protoplast or protonema of *B. argenteum* were ground to a fine powder using polishing stone and suspended in extraction buffer [50 mM Tris, 50 mM NaCl, 10% glycerinum 0.1% Tween 20, pH 7.4, 20 mM β -mercaptoethanol]. The homogenates was lysed on ice for 30 min and the lysis was accelerated by gentle shaking at 15min intervals. Cleavage products were centrifuged at 16,000 \times g for 15 min at 4°C and total protein was separated by 10% SDS-PAGE and blotted to a PVDF membrane (Merk Millopore, Ireland). The membrane was subjected to immuno-blot analysis using anti-green fluorescent protein antibody (ABclonal, United States) or anti-tubulin antibody (Sigma), and then HRP-conjugated anti-mouse IgG (Huaxingbio, China). Anti-GFP antibody was used to detect Citrine because of its high similarity to GFP (Griesbeck et al., 2001). The blot was analyzed using SuperSignal Chemiluminescent Substrates (BOSTER) and CHAMPCHEMI™ Chemiluminescent Imaging System (SINSAGE, China).

Confocal Microscopy

Transient expressed GFP signals in 16 h protoplast cells and stable transfection transgenic lines protonema cells were observed by a laser scanning confocal microscope (LSM780; Zeiss). GFP fluorescence was excited by a laser at 488 nm and chlorophyll was excited by 550 nm laser (Ahn et al., 2018).

PEG-Mediated Transfection and Analysis of Transgenic Lines

The MMM solution and PEGT solution were sterilized by filtration with 0.22 μ m bottle top filter to assure stability of pH and osmolarity. Then, 300 μ L of protoplast suspension was added to each tube with plasmid and gently mixed at room temperature for 15 minutes. Next, 300 μ L of PEGT solution was added to each tube and gently mixed until the solution became homogeneous. The mixture was then heat shocked at 45°C for 5 minutes, followed by 10 minutes of recovery at 20°C with gently shaking on a shaker. During this time, the cooled ABCG solution was prepared. 300 μ L of the ABCG solution was added to each tube every 2 minutes, total five times. Then, 1 mL of the ABCG solution was added to each tube seven times every 3 minutes. After each addition, the mixture solution was gently mixed to make the final

volume of the solution 9 mL (the process should be done gently and slowly by shaking back and forth). The transformation mix was wrapped in tin foil to avoid light and gently shaken for 1 hour at room temperature. The mixture was then centrifuged at 14°C for 2 minutes at 200 g, and the supernatant was aspirated using a 5 mL pipette tip and discarded. Next, 9 mL of PRMT (0.3% agar) culture medium was added to resuspend the protoplasts. The resuspended protoplasts were spread on PRMB culture dishes with glass paper, with about 2-3 mL of the mixture per dish. The plates were then cultured under full sunlight at 22±1°C (Supplementary Figure S1).

After nine days of culture following the PEG transformation of protoplasts, the material is transferred to BCDG medium containing 25 ng/uL G418 resistance and grown at 22±1°C under continuous light. After seven-day screenings, the surviving material is transferred to a standard BCDG medium and grown under the same conditions. When single plant growth is visible to the naked eye, the surviving strains are identified as positive transformation strains and await identification.

Results

The Sterilization of *B. argenteum*

Because moss leaves have only one layer of cells, it is difficult to get the sterilized moss. To obtain sterile materials, NaClO was used to detoxify the gametophyte materials collected from the wild. We explored the effect of NaClO treatment time on the sterilization efficiency of *B. argenteum*. The results showed that 5 minutes of treatment with 5% NaClO had the best sterilization effect. Treated with 5% NaClO for 5 min, the gametophyte was grown on sterile culture media, *B. argenteum* became lighter in color. After several days of cultivation, almost all the materials became whitened and died. Still, after seven days, new green filamentous structures could grow from the top of some stems and leaves under a dissecting microscope (Fig. 1A). We divided the sterilization status of each stem tip into three categories: sterilization leading to the death of the entire plant, survival with bacterial growth, and survival without bacterial growth. The rates of sterilization and survival of *B. argenteum* were obtained (Fig. 1B).

An Efficient Method for the Protonema of *B. argenteum* Using Liquid BCD with Ammonium Tartrate as additional N sources

Some gametophyte shoots were taken about 4 mm into liquid BCD medium with or without additional N or C sources. In liquid culture, the protonema cells grow from gametophyte stem and leaves and form fuzzy balls. As shown in (Fig. 1C), on the 7th day of liquid culture, the gametophytes with additional carbon sources developed new gametophyte. In contrast, the samples without carbon sources mainly remain in the original filamentous phase. Continuing to culture until the 14th day, the gametophytes with added carbon sources grow longer, and the spherical bodies become more extensive. In contrast, the samples without carbon sources remain filamentous. After 21 days of culture, the spherical bodies of the two groups with added carbon sources continue to grow, and the number of gametophytes increases further. However, the gametophytes with added carbon and nitrogen sources are covered with more original protonema. The spherical bodies of the two groups without added carbon sources continue to

grow larger, and more original protonema emerge. The sample with added nitrogen source but no carbon source has a much larger diameter, the longest original protonema, and almost no stem and leaf tissues, indicating that glucose promotes the development of protonema into gametophytes. Similar to overapplication of nitrogen (N) fertilizer delaying flowering in angiosperm (Yuan et al., 2016), ammonium tartrate as N sources inhibits moss development and can maintain moss at the protonema stage.

The Filaments of *B. argenteum* Can Survive Up to 95.42% Water Loss

This typical drought-tolerant moss resurrection plant can achieve dehydration of more than 95% and rapidly recover within a few seconds when rehydrated. The filaments of *P. patens* only can survive up to 92% water loss but cannot recover from complete desiccation (Frank et al., 2005; Khandelwal et al., 2010). It was reported that *P. patens* was desiccated inside a laminar flow hood for 24 h, but the rate of water loss is instability because of the different levels of humidity in different places (Khandelwal et al., 2010). Still, this method cannot guarantee the experimental material's dehydration level each time. We first attempted to use silica gel to dehydrate the material and observed the level of dehydration and stability. In the experiment, protonema material was selected. First, an excess amount of 5 cm in height of silica gel was added to a crystallization dish. Then the 7-day-old homogeneous slurry subculture material was transferred onto the silica gel in the crystallization dish and air-dried on a clean bench. The water loss rate of the material was measured at regular intervals (the weight of the filter paper was obtained after weighing the material, the filter paper was scraped clean after drying the material, and the weight of the filter paper was obtained after drying it under the same conditions). The results showed that the dehydration rate of the moss reached 95.42% (Supplementary Table S2). In order to test whether the moss material could revive after rehydration after the condition of extremely dehydration, we placed the dehydrated *B. argenteum* material into BCD medium after rehydration and grew it for one week, and found that the plants could grow normally. This indicates *B. argenteum* has a strong drought resistance and the ability to rapidly recover to the normal state after rehydration.

Identification and Molecular Phylogenetic Analysis of *B. argenteum*

With the development of molecular genetics, more and more molecular markers are used for species identification and classification. Some molecular markers can be used for the identification and classification of mosses. We used three molecular markers (trnL-F, trnG, atpB-rbcL) on the chloroplast genome and a molecular marker (nad5) on the mitochondrial genome, and two fragments of the 26S gene in nuclear to identify *B. argenteum*. The lengths of the sequenced molecular markers were 520 bp, 638 bp, 684 bp, 1976 bp and 1132 bp, 1095 bp, respectively. Sequencing results for other species can be obtained from GenBank. The concatenated sequences of these five molecular markers were used to construct a phylogenetic tree using the Maximum likelihood method using IQ-TREE program, and *B. argenteum* was found to be most closely related to reported *B. argenteum* Hedw (Pedersen et al., 2007), indicating that *B. argenteum* also belongs to the Bryaceae branch (Fig. 2).

Material Selection and Genome Size Determination

Although the transcriptome data of *B. argenteum* was reported (Gao et al., 2015; Gao et al., 2017), but the genome size of this plant is still uncertain. The genome size of *B. argenteum* CNU51 is 313 Mb using k-mer (Supplementary Figure S2). The genome size of CNU51 is smaller than 700 Mb reported (Wang, 2016), which suggests different *B. argenteum* populations might have the different genome ploidy type. *B. argenteum* CNU51 has a relatively small genome, making it a good model material for subsequent experiments. While, the moss model *P. patens* with about 500 Mb genome size has a disadvantage for that it has experienced multiple events of polyploidization during evolution that has resulted in a number of families of duplicated genes and functional redundancy (Rensing et al., 2008).

Protoplast Isolation of *Bryum argenteum* from Protonema and Protoplast Regeneration

The 15-day-old protonema tissues in liquid were used to isolate protoplasts. Protonema were pre-incubated for 1 h in 0.5 M mannitol with slow rotation. As the enzymatic digestion time increased, the cell walls were gradually broken down, and the protoplasts were gradually separated, increasing the number of protoplasts. At 100 minutes, there were almost no protoplasts in the field of view (Fig. 3A **a-l**). Counting the number of protoplasts isolated at different treatment times showed that the longer the breakdown time, the more protoplasts were isolated (Fig. 3B). The protoplasts produced after breakdown showed intense activity after FDA staining (Fig. 3C).

We chose BCDG solid medium containing 8% mannitol for protoplast regeneration and used a single cell to illustrate the different stages of protoplast regeneration. The process of protoplast regeneration in *Bryum argenteum* is similar to that of other mosses observed under a microscope. First, the protoplast regenerates a cell wall (Fig. 4A **a-b**), and injured cells will die within 1–2 days. From days 2 to 5, cells with newly formed cell walls divide into 2–3 cells (Fig. 4A **c-f**). By day 10, they further develop into new protonema (Fig. 4A **g-i**). Young gametophytes are visible to the naked eye at 20 days (Fig. 4A **j**).

After protoplast differentiation and cell wall formation, the protoplasts begin to differentiate. about 50% of the cells divide into two, with one cell ceasing division and only the other cell dividing to produce the next daughter cell. After several days, it grows into a single filamentous cell (Fig. 4B **a**). 23% of the cells produce two daughter cells with equal division ability, each of which subsequently divides independently. Ultimately, one protoplast cell grows into two filaments (Fig. 4B **b**). A small number of cells divide twice, producing three or four daughter cells, but only one or two of these daughter cells continue to divide into single filaments, while the other cells cease division (Fig. 4B **c-d**). From the statistical results, it can be seen that the splitting mode of splitting into two is the most common (Fig. 4C). The phenomenon of initial division during protoplast regeneration is very similar to spore germination.

Transient Transfection of Protoplasts via PEG-Mediated and Screening of *B. argenteum* Stable Transformation Strains

To establish a transformation system for *B. argenteum*, we firstly explored suitable transformation conditions using a transient expression system. We directly transformed the protoplasts of *B. argenteum* with the pCambia1302:GFP and evaluated the transformation and transient expression efficiency. The

PEG-mediated transformation method was based on the method of *P.patens*. After transformation, the regenerated cells were cultured on a liquid BCDG medium containing 8% mannitol for 16h. To assess the transient transformation efficiency, we observed GFP fluorescence. GFP fluorescence was dispersed throughout the cytoplasm after 16 hours of transient transformation with pCambia1302:GFP (Fig. 5A). At the same time, we used the method mentioned above to transform the pCambia1302:GFP into the protoplasts of the *B.argenteum*. After transformation, the regenerated cells were cultured on a solid BCDG medium containing 8% mannitol for ten days. Then, the screened cells were transferred to a hygromycin-containing medium at a 25 ug/mL concentration for the first seven-day selection round. After that, the recovered cells were transferred to a drug-free medium for growth recovery. Ten days later, they were transferred to a BCDG medium containing 50 ug/mL hygromycin for the second selection round. After five days of the second selection, almost all *B.argenteum* cells turned white and died. We obtained seven resistant plants. PCR analysis confirmed that seven plants contained the GFP fragment. Meanwhile, the expression of GFP was observed in the stable transformed positive plant *35S:GFP#2* (Fig. 5B). To examine chromosomal integration of transgenic constructs in transgenic lines, we assessed GFP transgene expression by semi-quantitative RT-PCR real-time quantitative PCR (Fig. 5C&S4). Next, the ectopic expression of Citrine protein was examined by immuno-blot assay. Anti-green fluorescent protein (GFP) antibody was used to detect Citrine because of its high similarity to GFP (Fig. 5D). These results indicate that the transfection method described here can be used to generate CNU51 transfectants.

Establishment of CRISPR/Cas9 Knockout System in *B.argenteum*

Based on the transcriptome data of *B.argenteum* (Gao et al., 2015; Gao et al., 2017) and our unpublished genome data of *B.argenteum*, we retrieved two homologous sequences of *ABI3* and named them *BaABI3A* and *BaABI3B*. We constructed a phylogenetic tree using the maximum likelihood method (ML) with the cloned amino acid sequences of *ABI3* in moss. The phylogenetic analysis showed that mosses formed one branch, and seed plants, including *Arabidopsis thaliana*, *Populus trichocarpa*, and rice, formed another branch, with the three homologous genes of the *AFL* subfamily in rice and *FUS3* forming a separate branch. *BaABI3A* and *PpABI3C* clustered in the moss branch, while *BaABI3B* clustered with *PpABI3A* and *PpABI3B* (Supplementary Figure S3). Comparative analysis of the phylogenetic tree and sequence proved that there are two homologous genes of *ABI3* in the *B.argenteum*, which belong to the *ABI3* family. To investigate the functions of the two *BaABI3* genes in *B.argenteum*, we explored their expression patterns under various stress treatments. We selected CNU51 progeny cultures growing for nine days as the source material. We subjected them to four non-biological stress conditions, namely 10 μ M ABA, 300 mM mannitol, drought/rehydration, and 250 mM NaCl. Under ABA stress treatment, the *BaABI3A* gene responded first, and its expression reached its maximum level in 2 hours, while the *BaABI3B* gene reached its maximum expression level in 8 hours. Under drought/rehydration treatment, both *BaABI3* genes were highly expressed under drought/rehydration treatment, with *BaABI3A* mainly expressed during the drought stress period and *BaABI3B* primarily expressed during the rehydration period after the drought. The response and expression patterns of the two *BaABI3* genes to salt stress were different, with *BaABI3A* being expressed in the later stages and *BaABI3B* being expressed in the earlier stages. Both *BaABI3* genes responded to osmotic stress caused by mannitol more slowly (Fig. 6A).

Currently, no reports of the CRISPR/Cas9 gene editing system in *B. argenteum*. Here, we used the CRISPR/Cas9 gene editing method from *P. patens* (Collonnier et al., 2016) to explore its application in *B. argenteum*. Using CNU51 moss as the material, we targeted two sites for *BaABI3A*, sgRNA 1 and sgRNA 2. Four mutant plants, *Baabi3a-5*, *Baabi3a-14*, *Baabi3a-20*, and *Baabi3a-21* were obtained through screening with the G418 antibiotic and sequencing identification. For *BaABI3B*, six target sites were designed, sgRNA 3, sgRNA 4, sgRNA 5, sgRNA 6, sgRNA 7, and sgRNA 8, and two mutant plants, *Baabi3b-16* and *Baabi3b-36* were obtained through screening with the G418 antibiotic and sequencing identification (Fig. 6B). We attempted different combinations of sgRNAs and found that only the plasmids containing sgRNA 1 and sgRNA 4 underwent gene editing. The statistical results showed that the editing efficiency of the *BaABI3A* gene in *B. argenteum* was 4.5%, and the editing efficiency of the *BaABI3B* gene was 1.9%. This result provides us with confidence to further explore the functions of other genes in *B. argenteum* (Table 1).

Table 1
Targeting efficiency of genome editing on *BaABI3A* and *BaABI3B* gene using the CRISPR-Cas9 system in *Bryum argenteum*

Gene	sgRNA used for transformation	G418 clones [□]	Number of analysed clones [†]	GT efficiencies (%) [‡]
<i>BaABI3A</i>	sgRNA1	89	4	4.5
<i>BaABI3B</i>	sgRNA4	103	2	1.9

sgRNA1 and sgRNA4 target *BaABI3A* and *BaABI3B* genes respectively (see Supplementary Table S3).

G418 clones are the stable antibiotic-resistant clones that survived after subculture on G418 medium.

Number of analysed clones[†] where the donor DNA template have been edited with deletions or insertions.

GT efficiencies (%) [‡]express the frequency of edited clones among the population of antibiotic-resistant transgenic clones.

There are no relevant literature reports on drought, salt stress, and osmotic stress treatment conditions in *B. argenteum*. Therefore, *BaABI3* gene mutants were used to explore the tolerance of *B. argenteum* to various abiotic stresses. A gradient of 100 mM, 200 mM, and 400 mM NaCl was set to analyze the optimal concentration for NaCl stress treatment. We found that wild-type and mutant strains could grow well under low-concentration salt treatment for three days and then transferred to a standard BCDG medium, which indicates that *B. argenteum* material is tolerant to short-term low-concentration salt stress. After two days of growth on BCDG medium containing 400 mM NaCl, *Baabi3a* *Baabi3b* mutant and wild-type *B. argenteum* materials appeared whitish, indicating significant salt stress. When transferred to a normal culture medium, the wild-type could recover the growth. In contrast, *Baabi3a-14* mutant strain could also recover growth (subsequent repeated experiments showed that *Baabi3a-14* could only partially recover growth, and its status was not as good as that of the WT plants, while

Baabi3a-5, *Baabi3a-20*, and *Baabi3a-21* mutant strains could only partially or not recover growth, showing a salt-sensitive phenotype) (Supplementary Figure S5).

To determine whether wild-type and mutants have salt-sensitive phenotype of *B. argenteum*, we treated the original prostrate material of the wild-type and mutants with 500 mM NaCl. The experimental results showed that the material treated directly with 500 mM NaCl turned white after 2 days of growth on the medium. The mutant strains *Baabi3a-5*, *Baabi3a-14*, and *Baabi3b-16* did not recover or only partially recovered during the recovery process. The results showed that the *ABI3* genes have the function in tolerating salt stress (Fig. 6C).

B. argenteum is a typical desiccation-tolerant (DT) plant. In this study, drying treatment was also performed on five mutants (*Baabi3a-5*, *Baabi3a-14*, *Baabi3a-20*, *Baabi3a-21*, *Baabi3b-16*) and the wild-type. Rehydration after 24 hours of drought, it was observed that the wild-type materials were able to survive, while only a little portion of the mutants resumed growth compared to the control. These results indicate that the *Baabi3a* and *Baabi3b* mutants are sensitive to drought stress, and both gene *BaABI3A* and *BaABI3B* function in desiccation for *B. argenteum* protonema (Fig. 6D)

Discussion

Moss plants are small and have a simple structure, making them the second largest group of existing land plants (Wang et al., 2022). The gametophyte of moss plants is leaf-like tissue or differentiated into root-like, stem-like, and leaf-like structures. This structure is intermediate between green algae and vascular plants, so moss plants are considered to have appeared shortly after the origin of land plants (Bowman et al., 2017; Christenhusz & Byng, 2016). Therefore, the phylogenetic position of mosses, liverworts, and hornworts in terrestrial plants is receiving increasing attention (Donoghue et al., 2021). For over two decades, *P. paten* has been developed and used as a model species for comparative studies in plant biology, widely applied in early land plant gene function research. The publication of its genome sequence has stimulated genetic studies (Rensing et al., 2008). The availability of various functional genetic tools, such as single gene knockout in *Physcomitrium patens*, has been effectively achieved through gene targeting due to its high homologous recombination rate and easy protoplast transformation (Schaefer, 2001; Schaefer & Zryd, 1997). In addition, the haploid state of most of the *P. patens* life cycle and its stem cell potential (Prigge & Bezanilla, 2010) have facilitated the study of *P. patens* genes and mutants. Recently, the use of sequence-specific nucleases, particularly the clustered regularly interspaced short palindromic repeats (CRISPR) and CRISPR-associated (Cas) system (Makarova et al., 2015), has been employed for gene targeting in different organisms (Wright et al., 2016). In nonvascular plants, the CRISPR-Cas9 system has been used in *Marchantia polymorpha* (Sugano et al., 2014) and *P. patens* (Collonnier et al., 2016). However, the CRISPR-Cas9 system has not been applied in *B. argenteum*.

In this study, we successfully established their sterile culture and hydroponic systems of *B. argenteum*. *B. argenteum* is one of the most desiccation tolerant (DT) moss species (Wood, 2007). We found that

dehydration capacity of its protonema reached about 95%, and *B. argenteum* protonema could grow normally after rehydration, demonstrating the high tolerance of *B. argenteum* (Fig. 1). *P. patens* can survive up to 92% water loss, but cannot recover from complete desiccation (Khandelwal et al., 2010). In addition, using molecular markers *trnL-F*, *trnG*, *atpB-rbcL*, *nad5*, and *26S* for molecular systematics analysis, we determined the phylogenetic position of *B. argenteum* in the genus *Bryum* (Fig. 2). Next, to establish a genetic transformation method for *B. argenteum*, we first determined the time of protoplast isolation and the state of protoplast redifferentiation. The results showed that the longer the collapse time, the more protoplasts could be isolated, but the activity of the protoplasts decreased after 60 minutes. Therefore, the digestion time was controlled within 60 minutes (Fig. 3). The regeneration process of protoplasts of *B. argenteum* is similar to that of monospores (Fig. 4). The enzyme concentration, mannitol concentration, and antibiotic concentration involved in the transformation process were consistent with those for *P. patens*, the concentration of mannitol was 8%, and the antibiotic screening concentration was 25 µg/mL. However, the concentration of enzymes was 0.8% in *B. argenteum*, which is higher than 0.5% of *P. patens* (Cove et al., 2009a). Maybe the cell wall components in different species is different, the concentration of driselase enzymes required varies (Roberts et al., 2012).

Polyethylene glycol (PEG)-mediated protoplast transformation is a routine method for studying nuclear gene function in moss plants (Nomura et al., 2016). We modified the transformation method of *P. patens* to achieve transient transformation and stable genetic transformation of *B. argenteum* by using pCambia-1302: GFP vector. Microscopic observation of the protoplasts and filamentous material showed stable fluorescence signals (Fig. 5). With the development of CRISPR/Cas9 technology and the high efficiency of gene editing, this study is the first attempt to use the CRISPR system for gene editing in *Bryaceae*. The CRISPR/Cas9 system was used for genetic transformation in *B. argenteum*, and surviving positive strains were identified after 6 weeks of selection and screening. The statistical results showed that the transformation efficiency of *B. argenteum* was about 1.9–4.5% (Table 1). The transformation efficiency of *B. argenteum* was lower than that of *P. patens* (Collonnier et al., 2016). It may be that CRISPR/Cas9 is not the optimal choice for the transformation of *Bryaceae*. Further, the adjustment of promoter in sgRNA and the improvement of Cas9 cleavage efficiency are the directions of our efforts. We can also try other gene editing system to find the most appropriate editing method for *B. argenteum*. To some extent, CRISPR's gene editing system applies to *B. argenteum*, which promotes the exploration of gene function in *B. argenteum* and enriches the understanding of the molecular biology of mosses. The experimental results above demonstrate the feasibility of the genetic transformation of *B. argenteum*, which lays a solid foundation for the future genetic transformation of more mosses and helps to identify more molecular functions of mosses, enriching the molecular mechanism of mosses.

Currently, *ABI3* plays an important regulatory role in cell maturation and plant development processes such as quiescence of shoot apical meristem and regulation of flowering time (Rohde et al., 1999). *ABI3* has also been found at junctions of ABA-auxin signaling crosstalk during seed germination, lateral root formation, and stress physiological processes (Liu et al., 2013). In recent years, the role of *ABI3* has been extended from developmental to abiotic stress responses (Khandelwal et al., 2010). Here, *ABI3* also play

an essential role in the dehydration tolerance and salt stress tolerating of *B. argenteum* (Fig. 6). Perhaps the widespread global distribution of *Bryophytes* is closely related to the role of *ABI3* in stress.

Although *B. argenteum* has a long history of research, most studies have focused on its environmental adaptability and environmental indication, and the exploration of its genetic molecular mechanism is still limited (Greenwood et al., 2019). This is the first report on establishing a genetic transformation method for *B. argenteum*. Despite pioneering attempts to modify the genetic information of non-model mosses in establishing the method, gene modification methods still lag far behind those for flowering plants or *P. patens* (Byun et al., 2021). It is believed that with the advancement of sequencing and gene editing technologies, we will gradually improve *B. argenteum*' transformation methods and achieve higher efficiency. The results of this study will contribute to both basic and applied science, such as understanding mechanisms of extreme environmental adaptation and extracting useful substances from *B. argenteum*.

Statements & Declarations

Funding

This work was supported by grants from the Major Research Plan of National Nature Science Foundation of China (91631109 to Y.He), the General Program of National Natural Science Foundation of China (No.31970658 Y.He. and No.30971558 to Y.Hu.).

Competing Interests

The authors declare that the research was conducted in the absence of any commercial or financial relationships that could be construed as a potential conflict of interest.

Author Contributions

Y.Hu., F.B. and Y.He. conceived and designed the project. G.Z., R.S. F.L., and Y.Hu performed most of experiments and analyzed the data. Other authors assisted in experiments and discussed the results. F.L. and Y. Hu. Wrote the manuscript.

Acknowledgments

We thank Fabien Nogué (Institut Jean-Pierre Bourgin, National Institute for Agricultural Research, France) for providing the pAct-Cas9 and the pBNRF plasmid.

Data Availability

Raw Data of *B. argenteum* CNU51 resequencing were uploaded to the National Genomics Data Center (<https://ngdc.cncb.ac.cn/>) in the sample accession SAMC2820342 the project ID PRJCA017895.

References

1. Ahn MM, Oh TR, Seo DH, Kim JH, Cho NH, Kim WT (2018) Arabidopsis group XIV ubiquitin-conjugating enzymes AtUBC32, AtUBC33, and AtUBC34 play negative roles in drought stress response. *J. Plant Physiol.* 230, 73–79. <https://doi.10.1016/j.jplph.2018.08.010>
2. Bowman JL, Kohchi T, Yamato KT et al (2017) Insights into land plant evolution garnered from the *Marchantia polymorpha* genome. *Cell.* 171(2), 287–304.e15. <https://doi.10.1016/j.cell.2017.09.030>
3. Byun MY, Seo S, Lee J, Yoo YH, Lee H (2021) Transfection of Arctic *Bryum sp. KMR5045* as a model for genetic engineering of cold-tolerant mosses. *Front. Plant Sci.* 11, 609847. <https://doi.10.3389/fpls.2020.609847>
4. Griesbeck O, Baird GS, Campbell RE, Zacharias DA, Tsien RY (2001) Reducing the environmental sensitivity of yellow fluorescent protein. *J Biol Chem* 276:29188–29194. <https://doi:10.1074/jbc.m102815200>
5. Cove DJ, Perroud PF, Charron AJ, McDaniel SF, Khandelwal A, Quatrano RS (2009a) Isolation and regeneration of protoplasts of the moss *Physcomitrella patens*. *Cold Spring Harb. Protoc.* Pdb.prot5140. <https://doi.10.1101/pdb.prot5140>
6. Christenhusz MJM, Byng JW (2016) The number of known plants species in the world and its annual increase. *Phytotaxa.* 261, 201–217. <https://doi.10.11646/phytotaxa.261.3.1>
7. Collonnier C, Epert A, Mara K et al (2016) CRISPR-Cas9 mediated efficient directed mutagenesis and RAD51-dependent and RAD51-independent gene targeting in the moss *Physcomitrella patens*. *Plant Biotechnol. J.* 15(1), 122–131. <https://doi.10.1111/pbi.12596>
8. Chen K, Wang Y, Zhang R, Zhang H, Gao C (2019) CRISPR/Cas Genome Editing and Precision Plant Breeding in Agriculture. *Annu. Rev. Plant Biol.* 70, 667–697. <https://doi.10.1146/annurev-arplant-050718-100049>
9. Donoghue PCJ, Harrison CJ, Paps J, Schneider H (2021) The evolutionary emergence of land plants. *Curr. Biol.* 31(19), R1281–R1298. <https://doi.10.1016/j.cub.2021.07.038>
10. Frank W, Ratnadewi D, Reski R (2005) *Physcomitrella patens* is highly tolerant against drought, salt and osmotic stress. *Planta.* 220, 384–394. <https://doi.10.1007/s00425-004-1351-1>
11. Gao B, Zhang D, Li X, Yang H, Zhang Y, Wood AJ (2015) De novo transcriptome characterization and gene expression profiling of the desiccation tolerant moss *Bryum argenteum* following rehydration. *BMC Genom.* 16(1), 416. <https://doi.10.1186/s12864-015-1633-y>
12. Gao B, Li X, Zhang D et al (2017) Desiccation tolerance in bryophytes: the dehydration and rehydration transcriptomes in the desiccation-tolerant bryophyte *Bryum argenteum*. *Sci. Rep.* 7(1), 7571. <https://doi.10.1038/s41598-017-07297-3>
13. Greenwood JL, Stark LR, Chiquoine LP (2019) Effects of rate of drying, life history phase, and ecotype on the ability of the moss *Bryum argenteum* to survive desiccation events and the influence

- on conservation and selection of material for restoration. *Front. Ecol. Evol.* 7:388.
<https://doi.org/10.3389/fevo.2019.00388>
14. Gao C (2021) Genome engineering for crop improvement and future agriculture. *Cell.* 184 (6):1621–1635. <https://doi.org/10.1016/j.cell.2021.01.005>
 15. Hohe A, Egener T, Lucht JM, Holtorf H, Reinhard C, Schween G, Reski R (2004) An improved and highly standardised transformation procedure allows efficient production of single and multiple targeted gene-knockouts in a moss, *Physcomitrella patens*. *Curr Genet.* 44(6):339 – 47.
<https://doi.org/10.1007/s00294-003-0458-4>
 16. Hui R, Li X, Chen C et al (2013) Responses of photosynthetic properties and chloroplast ultrastructure of *Bryum argenteum* from a desert biological soil crust to elevated ultraviolet-B radiation. *Physiol Plantarum.* 147(4), 489–501. <https://doi.org/10.1111/j.1399-3054.2012.01679.x>
 17. He X, He KS, Hyvönen J (2016) Will bryophytes survive in a warming world? *Perspect. Plant Ecol. Evol. Syst.* 19, 49–60. <https://doi.org/10.1016/j.ppees.2016.02.005>
 18. Ikeda Y, Nishihama R, Yamaoka S et al (2018) Loss of CG methylation in *Marchantia polymorpha* causes disorganization of cell division and reveals unique DNA methylation regulatory mechanisms of non-CG methylation. *Plant Cell Physiol.* 59(12), 2421–2431. <https://doi.org/10.1093/pcp/pcy161>
 19. Livak. KJ, Schmittgen TD (2001) Analysis of relative gene expression data using real-time quantitative PCR and the 2(- Delta Delta C(T)) method, *Methods.* 402–408.
<https://doi.org/10.1006/meth.2001.1262>
 20. Khandelwal A, Cho SH, Marella H et al (2010) Role of ABA and ABI3 in desiccation tolerance. *Science.* 327(5965), 546. <https://doi.org/10.1126/science.1183672>
 21. Khandelwal A, Cho SH, Marella H, Sakata Y, Perroud PF, Pan A, Quatrano RS (2010) Role of ABA and *ABI3* in desiccation tolerance. *Science* 327 (5965), 546. <https://doi.org/10.1126/science.1183672>
 22. Liu X, Zhang H, Zhao Y, Feng Z, Li Q, Yang HQ (2013) Auxin controls seed dormancy through stimulation of abscisic acid signaling by inducing ARF-mediated ABI3 activation in *Arabidopsis*. *Proc Natl Acad Sci U S A.* 110 (38), 15485– 15490. <https://doi.org/10.1073/pnas.1304651110>
 23. Lopez-Obando M, Hoffmann B, Géry C et al (2016) Simple and efficient targeting of multiple genes through CRISPR-Cas9 in *Physcomitrella patens*. *G3 (Bethesda, Md.).* 6(11), 3647–3653.
<https://doi.org/10.1534/g3.116.033266>
 24. Marella HH, Sakata Y, Quatrano RS (2006) Characterization and functional analysis of ABSCISIC ACID INSENSITIVE3-like genes from *Physcomitrella patens*. *Plant J.* 46
25. –1044. [https://doi.org/10.1111/j.1365-313X\(2006\)02764.x](https://doi.org/10.1111/j.1365-313X(2006)02764.x)
 26. Makarova KS, Haft DH, Barrangou R et al (2011) Evolution and classification of the CRISPR-Cas systems. *Nat Rev Microbiol.* 9, 467–477. <https://doi.org/10.1038/nrmicro2577>
 27. Nomura T, Sakurai T, Osakabe Y, Osakabe K, Sakakibara H (2016) Efficient and heritable targeted mutagenesis in mosses using the CRISPR/Cas9 system. *Plant Cell Physiol.* 57, 2600–2610.
<https://doi.org/10.1093/pcp/pcw173>

28. Pedersen N, Holyoak DT, Newton AE (2007) Systematics and morphological evolution within the moss family Bryaceae: a comparison between parsimony and Bayesian methods for reconstruction of ancestral character states. *Mol Phylogenet Evol.* 43(3), 891–907. <https://doi.10.1016/j.ympev.2006.10.018>
29. Prigge MJ, Bezanilla M (2010) Evolutionary crossroads in developmental biology: *Physcomitrella patens*. *Development.* 137, 3535–3543. <https://doi.10.1242/dev.049023>
30. de Ponce I, Montesano M (2013) Activation of defense mechanisms against pathogens in mosses and flowering plants. *Int. J. Mol. Sci.* 14(2), 3178–3200. <https://doi.10.3390/ijms14023178>
31. Pisa S, Biersman F, Convey P, Patino J, Vanderpoorten A, Werner O (2014) The cosmopolitan moss *Bryum argenteum* in Antarctica: recent colonisation or in situ survival? *Polar Biol.* 37, 1469–1477. <https://doi.10.1007/s00300-014-1537-3>
32. Pandey VK, Mishra R, Chandra R (2014) In vitro culture of moss *Bryum coronatum* Schwaegr. (Bryaceae) and its phytochemical analysis. *Int J Pharm Pharmacol Sci* 6:307–311
33. Puttick MN, Morris JL, Williams TA et al (2018) The interrelationships of land plants and the nature of the ancestral embryophyte. *Curr. Biol.* 28(5), 733–745.e2. <https://doi.10.1016/j.cub.2018.01.063>
34. Rohde A, Van Montagu M, Boerjan W (1999) The ABSCISIC ACID-INSENSITIVE 3 (*ABI3*) gene is expressed during vegetative quiescence processes in *Arabidopsis*. *Plant, Cell Environ.* 22 (3), 261–270. <https://doi.10.1046/j.1365-3040.1999.00428.x>
35. Rensing SA, Lang D, Zimmer AD et al (2008) The genome of the moss *Physcomitrella patens* reveals evolutionary insights into the conquest of land by plants. *Science.* 319, 64–69. <https://doi.10.1126/science.1150646>
36. Roberts AW, Roberts EM, Haigler CH (2012) Moss cell walls: structure and biosynthesis. *Front. Plant Sci.* 3:166. <https://doi.10.3389/fpls.2012.00166>
37. Shaw J, Beer SC, Lutz J (1989) Potential for the evolution of heavy metal tolerance in *Bryum argenteum*, a moss. I. variation within and among populations. *Bryologist.* 92, 73–80. <https://doi.10.2307/3244019>
38. Shaw J, Albright DJ (1990) Potential for the evolution of heavy metal tolerance in *Bryum argenteum*, a moss. II. Generalized tolerances among diverse populations. *Bryologist.* 93, 187–192. <https://doi.10.2307/3243622>
39. Schaefer DG, Zrýd JP (1997) Efficient gene targeting in the moss *Physcomitrella patens*. *Plant J.* 11(6), 1195–1206. <https://doi.10.1046/j.1365-313x.1997.11061195.x>
40. Schaefer DG (2001) Gene targeting in *Physcomitrella patens*. *Curr. Opin. Plant Biol.* 4(2), 143–150. [https://doi.10.1016/s1369-5266\(00\)00150-3](https://doi.10.1016/s1369-5266(00)00150-3)
41. Sabovljević A, Sabovljević M, Grubišić D, Konjević R (2005) The effect of sugars on development of two moss species (*Bryum argenteum* and *Atrichum undulatum*) during in vitro culture. *Belg. J. Bot.* 138, 79–84. <https://doi.10.2307/20794569>
42. Sabovljević A, Sabovljević M, Grubišić D (2010) Gibberellin influence on the morphogenesis of the moss *Bryum argenteum* Hedw. In in vitro conditions. *Arch. Biol. Sci.* 62, 373–380.

<https://doi.10.2298/abs1002373s>

43. Schroeter B, Green TGA, Kulle D, Pannewitz S, Schlensog M, Sancho LG (2012) The moss *Bryum argenteum* var. *muticum* Brid. Is well adapted to cope with high light in continental Antarctica. *Anta. Sci.* 24, 281–291. <https://doi.10.1017/S095410201200003X>
44. Sugano SS, Shirakawa M, Takagi J et al (2014) CRISPR/Cas9-mediated targeted mutagenesis in the liverwort *Marchantia polymorpha* L. *Plant Cell Physiol.* 55(3), 475–481. <https://doi.10.1093/pcp/pcu014>
45. Sousa F, Foster PG, Donoghue PCJ, Schneider H, Cox CJ (2019) Nuclear protein phylogenies support the monophyly of the three bryophyte groups (*Bryophyta Schimp.*). *New Phytol.* 222(1), 565–575. <https://doi.10.1111/nph.15587>
46. Taberlet P, Gielly L, Pautou G, Bouvet J (1991) Universal primers for amplification of three non-coding regions of chloroplast DNA. *Plant Mol Biol.* 17(5):1105-9. <https://doi.10.1007/BF00037152>
47. Trouiller B, Charlot F, Choinard S, Schaefer DG, Nogué F (2007) Comparison of gene targeting efficiencies in two mosses suggests that it is a conserved feature of Bryophyte transformation. *Biotechnol. Lett.* 29(10), 1591–1598. <https://doi.10.1007/s10529-007-9423-5>
48. Takezawa D, Komatsu K, Sakata Y (2011) ABA in bryophytes, how a universal growth
49. regulator in life became a plant hormone? *J Plant Res.* 124, 437–453. <https://doi.10.1007/s10265-011-0410-5>
50. Trogu S, Ermert AL, Stahl F, Nogué F, Gans T, Hughes J (2020) Multiplex CRISPR-Cas9 mutagenesis of the phytochrome gene family in *Physcomitrium (Physcomitrella) patens*. *Plant Mol. Biol.* 107(4–5), 327–336. <https://doi.10.1007/s11103-020-01103-x>
51. Wood AJ (2007) The nature and distribution of vegetative desiccation-tolerance in hornworts, liverworts and mosses. *Bryologist.* 110, 163–177. [https://doi.10.1639/0007-2745\(2007\)110\[163:IENFIB\] 2.0.CO;2](https://doi.10.1639/0007-2745(2007)110[163:IENFIB] 2.0.CO;2)
52. Wiedemann G, Hermsen C, Melzer M et al (2010) Targeted knock-out of a gene encoding sulfite reductase in the moss *Physcomitrella patens* affects gametophytic and sporophytic development. *FEBS Lett.* 584(11), 2271–2278. <https://doi.10.1016/j.febslet.2010.03.034>
53. Wang C (2016) Measuring genome size in silver moss *Bryum argenteum* Hedw. By flow cytometry. *Molecular Plant Breeding (China).* 14(4), 858–863. <https://doi.10.13271/j.mpb.014.000858>
54. Wright AV, Nuñez JK, Doudna JA (2016) Biology and applications of CRISPR systems: harnessing nature’s toolbox for genome engineering. *Cell.* 164(1–2), 29–44. <https://doi.10.1016/j.cell.2015.12.035>
55. Wang QH, Zhang J, Liu Y et al (2022) Diversity, phylogeny, and adaptation of bryophytes: insights from genomic and transcriptomic data. *J. Exp. Bot.* 73(13), 4306–4322. <https://doi.10.1093/jxb/erac127>
56. Yuan S, Zhang ZW, Zheng C et al (2016) *Arabidopsis* cryptochrome 1 functions in nitrogen regulation of flowering. *Proc Natl Acad Sci U S A.* 113(27), 7661–7666. <https://doi.10.1073/pnas.1602004113>

57. Yin K, Gao C, Qiu J-L (2017) Progress and prospects in plant genome editing. *Nat. Plants*. 3, 17107. <https://doi.10.1038/nplants.2017.107>
58. Zhang Y, Liu X, Zhang K, Zhang D, Guan K (2018) An ABSCISIC ACID INSENSITIVE3-like gene from the desert moss *Syntrichia caninervis* confers abiotic stress tolerance and reduces ABA sensitivity. *Plant Cell*. 133, 417–435. <https://doi.10.1007/s11240-018-1394-9>
59. Zhao M, Li Q, Chen Z et al (2018) Regulatory Mechanism of ABA and ABI3 on vegetative development in the moss *Physcomitrella patens*. *Int. J. Mol. Sci.* 19(9), 2728. <https://doi.10.3390/ijms19092728>
60. Zhu H, Li C, Gao C (2020) Applications of CRISPR-Cas in agriculture and plant biotechnology. *Nat. Rev. Mol. Cell Biol.* 21, 661–677. <https://doi.10.1038/s41580-020-00288-9>
61. Zaccara S, Patiño J, Convey P, Vanetti I, Cannone N (2020) Multiple colonization and dispersal events hide the early origin and induce a lack of genetic structure of the moss *Bryum argenteum* in Antarctica. *Ecol. Evol.* 10(16), 8959–8975. <https://doi.10.1002/ece3.6601>

Figures

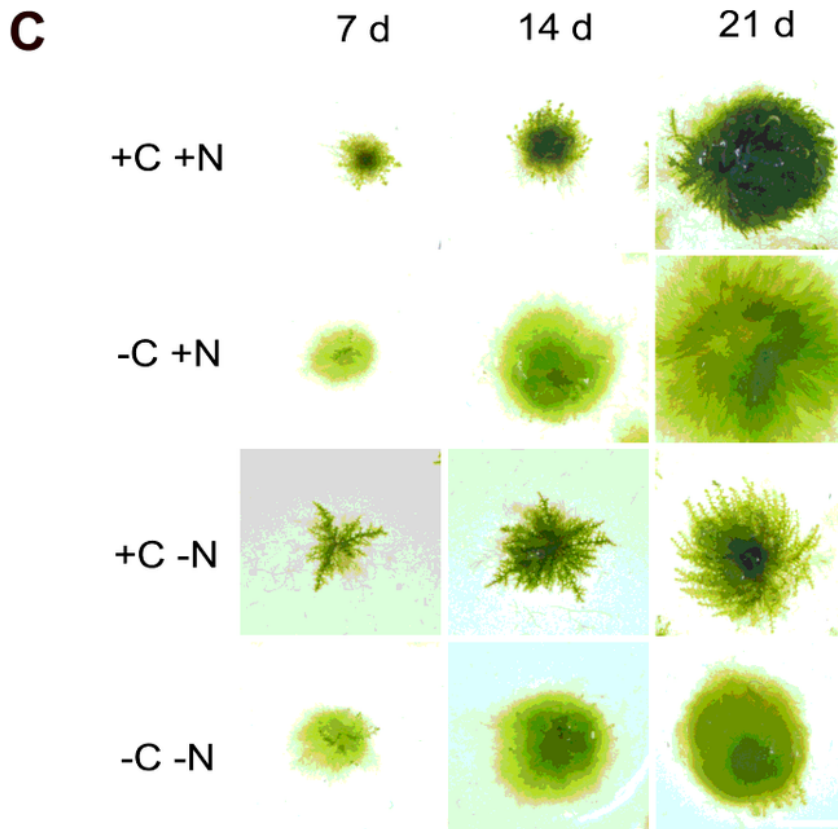
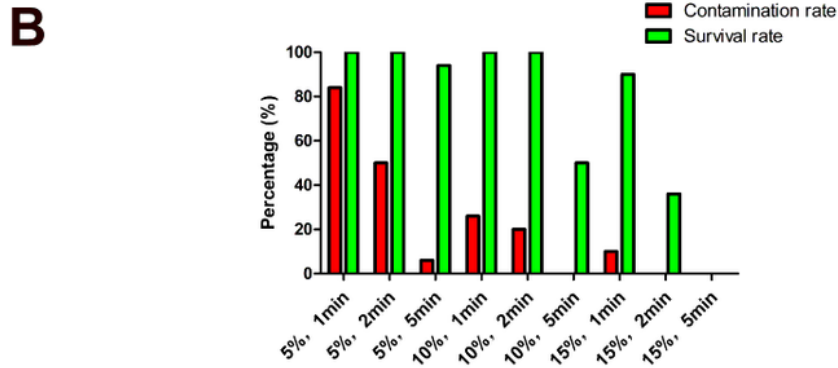
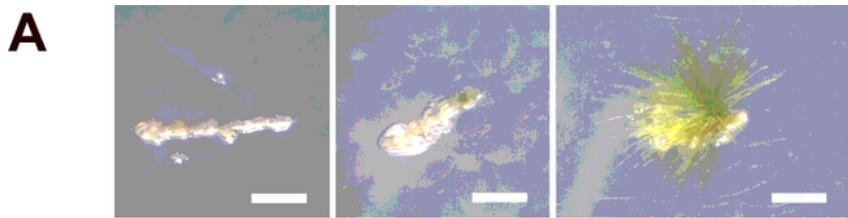


Figure 1

Establishment of aseptic culture system of *Bryum argenteum*. (A) Growth of aseptic seedlings after detoxification. (B) Effects of detoxification time and concentration on obtaining aseptic seedlings. (C) Cultivation of gametophytes on BCD medium with different carbon (C) and nitrogen (N) sources. Scale bar: 5 mm.

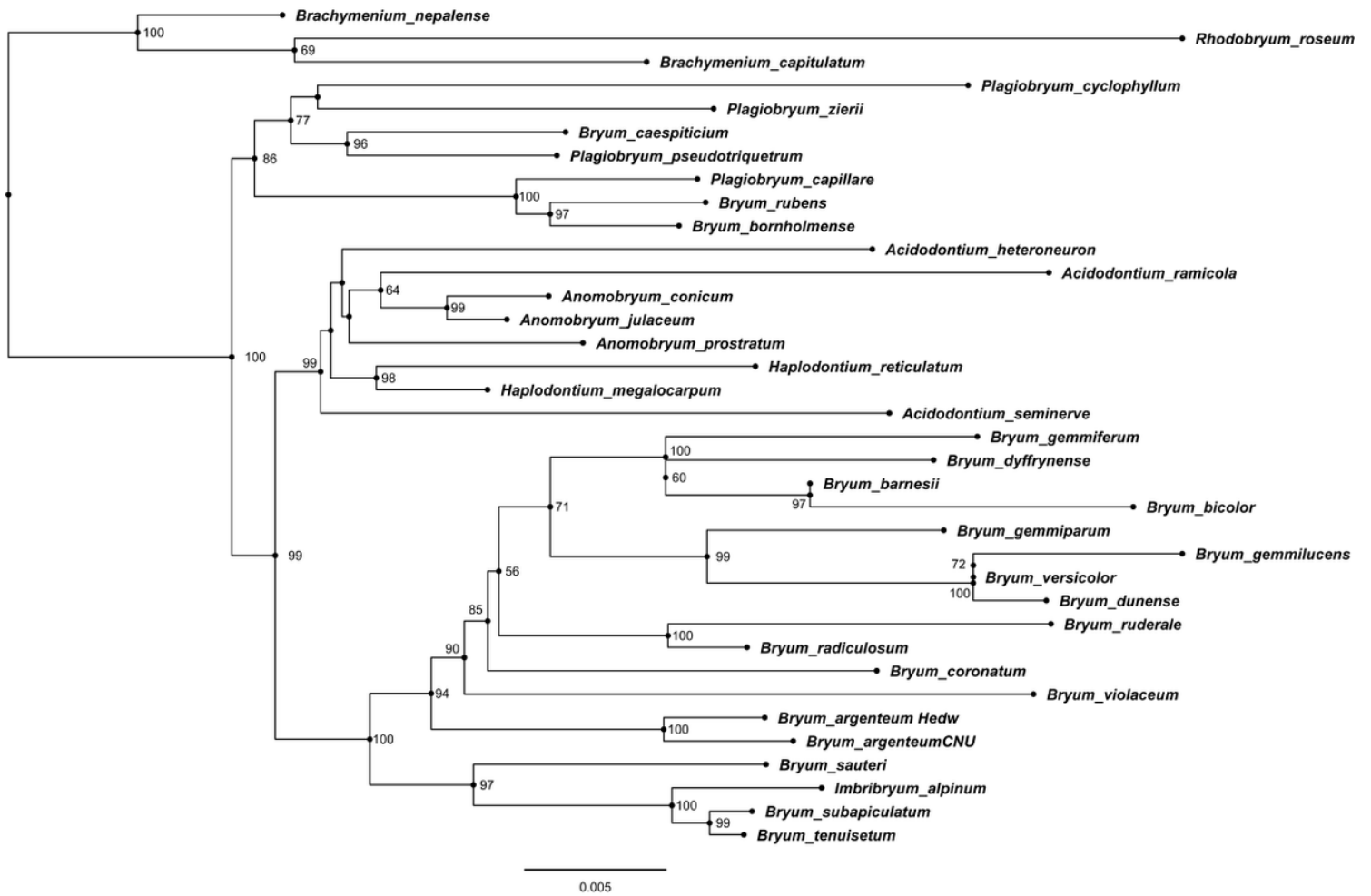


Figure 2

Molecular phylogenetic analysis of *Bryum argenteum*. Amplified trnL-F trnG atpB-rbcL nad5 and 26S sequences were aligned with sequences from other mosses and analyzed using the maximum likelihood method. The phylogenetic tree shows that *Bryum argenteum* is closely related to *Bryum argenteum* Hedw. Sequencing results for other species can be obtained from GenBank (Taberlet et al., 1991; Pedersen N et al., 2006 Table 1).

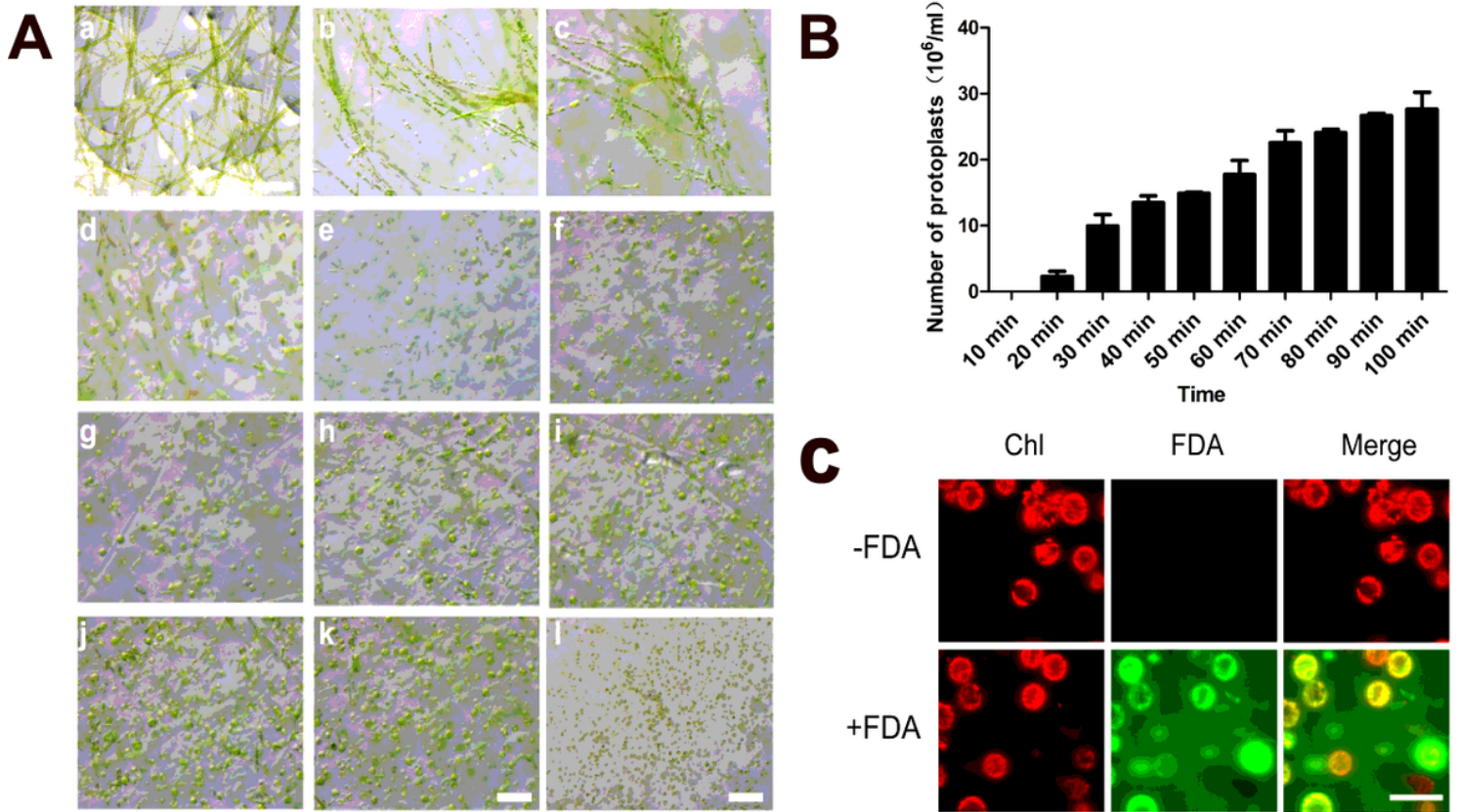


Figure 3

Production of protoplasts after treatment with cellulase for different times. (A) Production of protoplasts after treatment with cellulase for 0 min (a), 10 min (b), 20 min(c), 30min(d), 40 min(e), 50 min(f), 60 min (g), 70 min (h), 80 min (i), 90 min (j), 100 min (k), last(l). Scale bar: a = 0.4 mm, b-k = 0.2 mm, l = 0.5 mm. (B) Number of protoplasts under different treatment times in figure A. (C) Protoplast viability by FDA testing. Scale bar: 50 μ m.

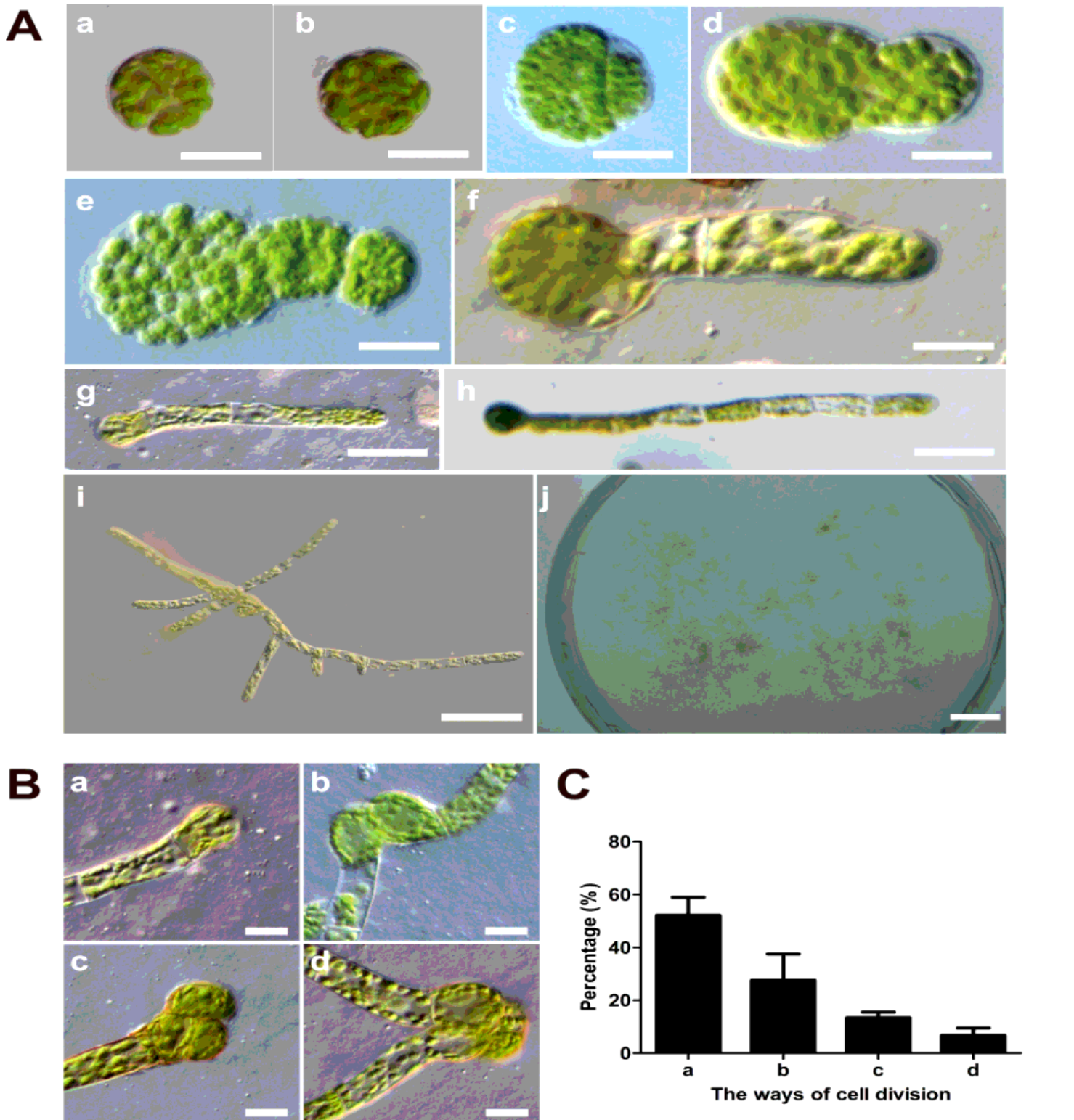


Figure 4

Cells division during the early stage of protoplast regeneration. (A) The cell division stage at 1 Day(a), 2 Day(b), 3 Day(c), 4 Day(d), 5 Day(e), 6 Day(f), 7 Day (g), 8 Day(h), 10 Day(i), 20 Day(j). Scale bars (a-f) 20 μ m; (g-h) 50 μ m; (i) 100 μ m; (j) 1 cm. (B) The cell division ways: Protoplast without division(a), Protoplast dividing into two cells(b), Protoplast dividing into three cells(c), Protoplast dividing into four cells(d). (C) Division pattern rate of protoplasts.

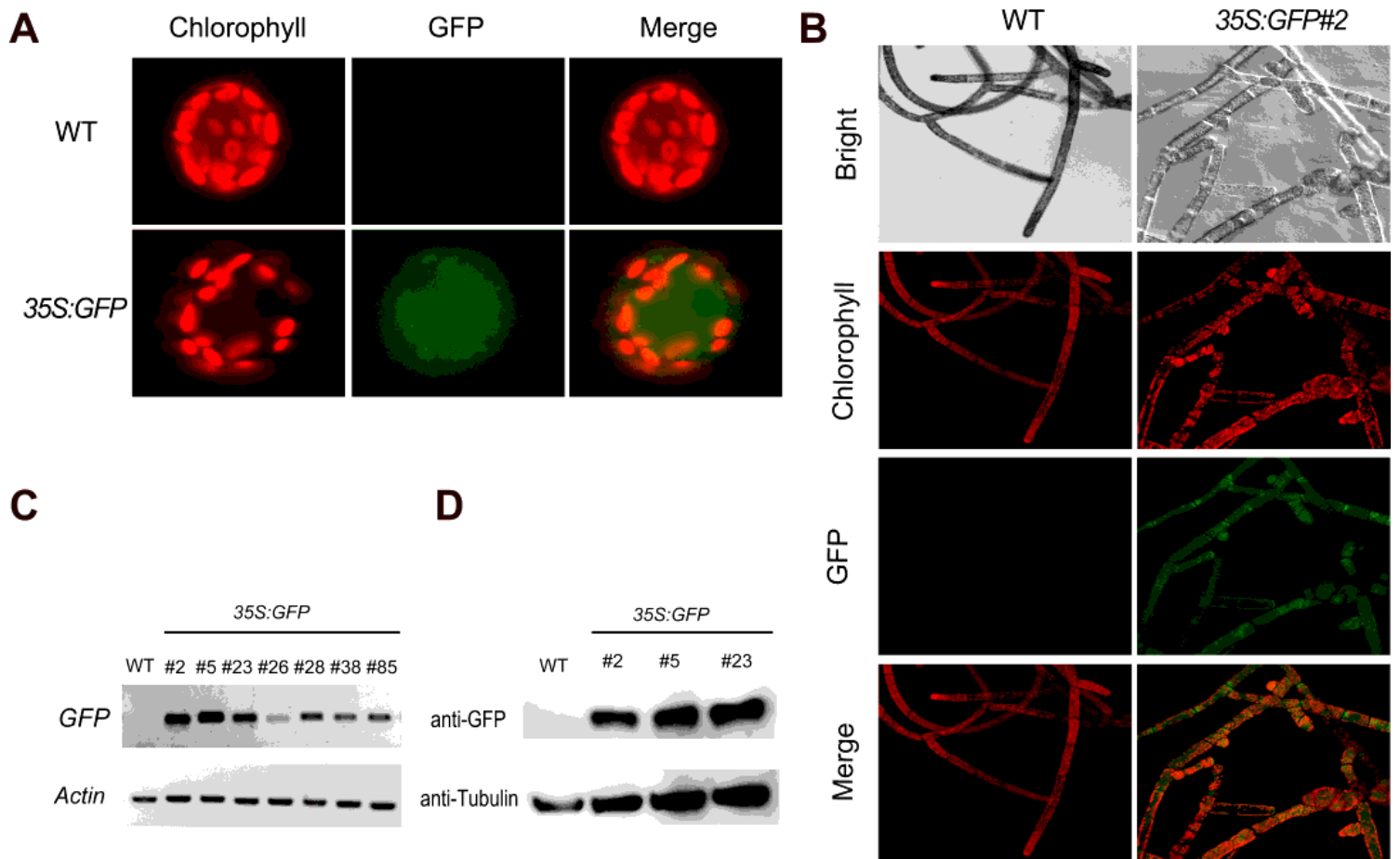


Figure 5

Gene expression analysis of transiently and stably transformed plants in *Bryum argenteum*. (A) Fluorescence observation of wild-type protoplasts and transiently GFP-transfected protoplasts. *35S:GFP* represents the transiently transformed pCambia-1302 plant. Scale bar: 10 μ m. (B) Fluorescence observation of wild-type protonema and stably GFP-transformed protonema. *35S:GFP#2* represents the stably transformed pCambia-1302 plant. Scale bar: 20 μ m. (C) Reverse transcription (RT)-PCR analysis of GFP expression in stably GFP-transformed protonema (#2 #5 #23 #26 #28 #38 #85). Actin was used as an internal control. (D) Immunoblot Analysis for GFP expression in transgenic lines. #2 #5 #23 represents the stably transformed pCambia-1302 plant. GFP was detected using anti-GFP antibody. Blot analyzed with anti-tubulin was used as an internal control.

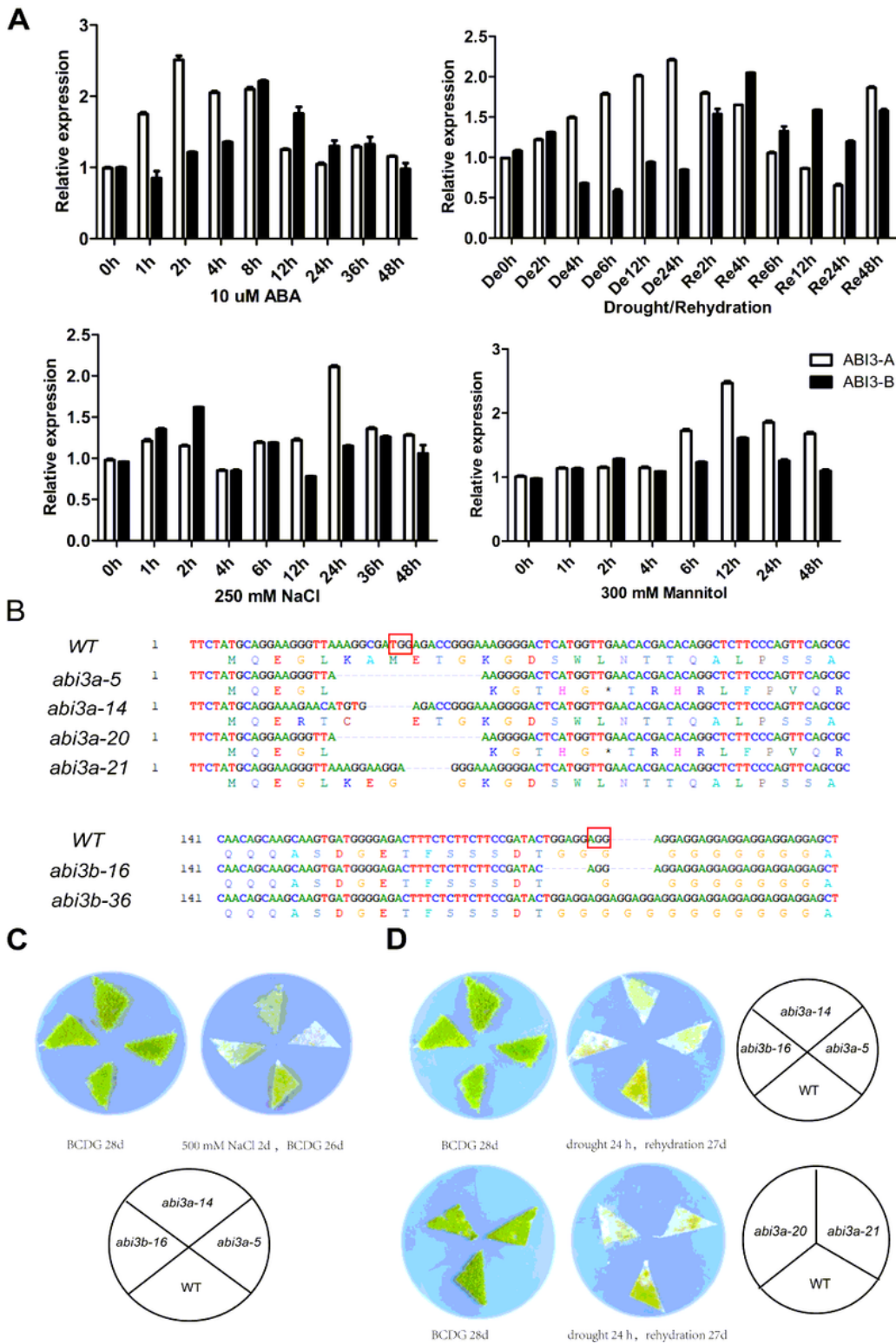


Figure 6

The phenotype of wild type and *Baabi3* mutants under NaCl stress and drought stress. (A) Expression patterns of *BaABI3* under various stress treatments. 10 μ M ABA stress (a), drought/rehydration stress (b), 250 mM NaCl stress (c), 300 mM Mannitol (d). (B) Sequence analysis of *Baabi3* mutants. Red borders indicate PAM sites. (C) Phenotypic analysis of mutants under salt stress. The plants were grown for 28 days on BCDG medium; then transferred to BCDG medium containing 500 mM NaCl and grown for 2

days, followed by another 26 days of growth on BCDG medium. (D) Phenotypic analysis of mutants under drought/rehydration stress. The plants were grown for 28 days on BCDG medium; then drought 24 h, finally rehydration 27 d.

Supplementary Files

This is a list of supplementary files associated with this preprint. Click to download.

- [Rawdata.rar](#)
- [SupplementaryMaterial202309.docx](#)